Journal of Zhejiang University-SCIENCE A (Applied Physics & Engineering)
ISSN 1673-565X (Print); ISSN 1862-1775 (Online)
www.zju.edu.cn/jzus; www.springerlink.com
E-mail: jzus@zju.edu.cn

Buckling response of offshore pipelines under combined tension, bending, and external pressure*

Shun-feng GONG†, Lin YUAN, Wei-liang JIN

(*Institute of Structural Engineering, Zhejiang University, Hangzhou 310058, China*)

†E-mail: sfgong@zju.edu.cn

Received Dec. 4, 2010; Revision accepted Mar. 21, 2011; Crosschecked July 4, 2011

Abstract: The buckle and collapse of offshore pipeline subjected to combined actions of tension, bending, and external pressure during deepwater installation has drawn a great deal of attention. Extended from the model initially proposed by Kyriakides and his co-workers, a 2D theoretical model which can successfully account for the case of simultaneous tension, bending, and external pressure is further developed. To confirm the accuracy of this theoretical method, numerical simulations are conducted using a 3D finite element model within the framework of ABAQUS. Excellent agreement between the results validates the effectiveness of this theoretical method. The model is then used to study the effects of several important factors such as load path, material properties, and diameter-to-thickness ratio, etc., on buckling behaviors of the pipes. Based upon parametric studies, a few significant conclusions are drawn, which aims to provide the design guidelines for deepwater pipeline with solid theoretical basis.

Key words: Deepwater, Offshore pipeline, Buckle, External pressure
doi:10.1631/jzus.A1000489 **Document code:** A **CLC number:** X703

1 Introduction

Submarine pipeline is an important part of offshore oil and gas exploitation projects. The installation of pipelines, especially in deep water, can induce rather severe loads to the structure, which, as a result, will lead to the unforeseeable risks and challenges. Pipes in the sag-bend region have to withstand combined tension, bending, and ambient pressure regardless of the installation method used (S-lay, J-lay or reeling-lay) (Kashani and Young, 2005; Li *et al.*, 2008). Under these combined loads, deepwater pipelines are vulnerable to local buckling, which will, in turn, have the potential of initiating a propagating buckle. Once the propagating buckle occurs, the pipeline will suffer from catastrophic flattening, resulting in failure of whole structure as well as huge economic loss.

The buckling response of the pipes subjected to installation loads is of paramount importance, and as a result this subject has received much attention in the past few decades. Gellin (1980) investigated the effect of nonlinear material behavior on the buckling of an infinitely-long cylindrical shell under pure bending. Subsequently, the response and stability of elasto-plastic circular pipes under combined bending and external pressure were analyzed by Kyriakides and Shaw (1982). They determined the maximum moment and curvature as a function of the material and geometric parameters for different pressures. Corona and Kyriakides (1988) further studied the stability of circular tubes under combined bending and external pressure. The curvature-pressure interaction collapse envelopes were generated for two different loading paths involving bending followed by pressure and pressure followed by bending. It was found that the loading path strongly affected buckling response of the tube, critical collapse loads, and the nature of instabilities. Dyau and Kyriakides (1992) developed a

* Project supported by the National Natural Science Foundation of China (No. 51009122), the Fundamental Research Funds for the Central Universities (No. 2010QNA4030), and the National High-Tech R&D (863) Program of China (No. 2006AA09A105)

2D model to examine the buckling response of tubes under combined bending and tension, in which two types of combined loadings were investigated in detail. Al-Sharif and Preston (1996) proposed a deterministic model to calculate the collapse of the tube under combined bending and pressure, and then developed a numerical model to simulate the plastic collapse of thick-walled pipe. Moreover, it was found that the simulation results agreed well with those of the deterministic model. Studies on the collapse of thick-walled tubes under three different load combinations, i.e., bending and pressure, tension and pressure, and tension and bending, were performed respectively by Kyriakides and Corona (2007). Numerical models with simultaneous tension, bending, and external pressure applied were carried out to simulate the behavior of thick-walled tubes using ABAQUS by Bai *et al.* (1997). They also proposed a set of interaction equations accounting for some major factors affecting collapse envelopes based on the analyses. Lately, Yuan *et al.* (2009) respectively investigated the buckling performance of deepwater pipes subjected to pure bending, and combined bending and external pressure. It is indicated that the buckling response of the tube is closely related to the diameter-to-thickness ratio, and the existence of initial curvature will weaken the load-carrying capacity of the pipe to resist external hydrostatic pressure.

The present study aims to extend the general theory proposed by Kyriakides and his co-workers to further investigate the buckling response of thick-walled tubes under simultaneous tension, bending, and external pressure. It is assumed that the buckling is symmetric about the vertical plane and deforms uniformly along the length of pipeline. Based upon the nonlinear ring theory, which could accommodate large deformation and circumferential extension scenario, the relationship of strain and displacement is obtained. Then, a virtual work approach is adopted to formulate a set of equilibrium equations, which are solved using the Newton-Raphson method. Meanwhile, a 3D numerical model is developed under the same loading conditions using ABAQUS, and comparison of the results between the two methods is carried out. It is found that the growth of ellipticity corresponding to theoretical model is somewhat slower when the applied loads are relatively high. Furthermore, the buckling response is studied in detail corresponding to a certain load path denoted $T\rightarrow$ Radial(κ, P), in which the pipe is first tensioned to a chosen value T in the longitudinal direction, and then the curvature κ and external pressure P are applied in proportion. This load path considered in the present study can more approximate the case of practical pipe-laying. Besides, a parametric study concerning several important influence factors was conducted, and some significant conclusions were drawn.

2 Theoretical formulations

2.1 Kinematics

The tube considered is a long, circular, thick-walled tube, with its mean radius R and thickness t. Uniform tension T, curvature κ and external pressure P are assumed to be applied along the length. As shown in Fig. 1, it is noted that the coordinate z is the radial distance from the mid-surface of the tube wall rather than from the centre, and the displacements of a point on the mid-surface are denoted as u, v and w with respect to axial, circumferential and radial coordinates x, θ and z, respectively. The plane sections are assumed to be normal to the mid-surface of the tube cross-section before and during deformation. Besides, small strain and finite rotations about the axes are assumed here (Gellin, 1980).

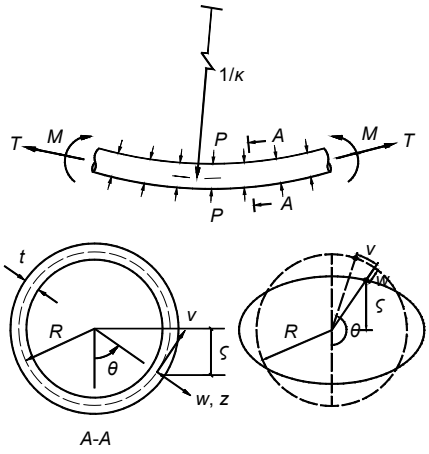

Fig. 1 Geometric parameters and coordinate system
ς is the distance from a point in the tube wall to the neutral axis; M is the bending moment

The axial strain of the tube can be denoted as

$$\varepsilon_x = \varepsilon_x^0 + \varsigma\kappa, \tag{1}$$

where ε_x^0 is the axial strain of neutral axis, ς is the distance from a point in the tube wall to the neutral axis, and can be obtained from Fig. 1:

$$\varsigma = (R+w)\cos\theta - v\sin\theta + z\cos\theta. \tag{2}$$

The circumferential strain can be expressed as

$$\varepsilon_\theta = \varepsilon_\theta^0 + z\cdot\kappa_\theta, \tag{3}$$

where

$$\varepsilon_\theta^0 = \left(\frac{v'+w}{R}\right) + \frac{1}{2}\left(\frac{v'+w}{R}\right)^2 + \frac{1}{2}\left(\frac{v-w'}{R}\right)^2, \tag{4}$$

and

$$\kappa_\theta = \left(\frac{v'-w''}{R^2}\right) \Bigg/ \sqrt{1-\left(\frac{v-w'}{R}\right)^2}, \tag{5}$$

where $()'$ denotes the differential with respect to θ.

2.2 Constitutive model

The material of deepwater pipelines exhibits good plastic deformation capacity, and the pipe can be modeled as an elastoplastic solid. The Ramberg-Osgood model is used to characterize nonlinear stress-strain relationships of the material shown in Fig. 2, which is given as

$$\varepsilon = \frac{\sigma}{E}\left[1+\frac{3}{7}\left|\frac{\sigma}{\sigma_y}\right|^{n-1}\right], \tag{6}$$

where E is Young's modulus, σ_y is the effective yield stress, and n is the material hardening parameter.

The incremental J_2 flow theory of plasticity with isotropic hardening is used to model the plastic behavior of material. The radial stress σ_r and shear stress $\{\sigma_{x\theta}, \sigma_{\theta r}, \sigma_{rx}\}$ are neglected due to the fact that these components are quite small when comparing with those in the axial and circumferential directions. Therefore, the incremental constitutive model can be simplified into:

$$\begin{Bmatrix}\dot\varepsilon_x\\ \dot\varepsilon_\theta\end{Bmatrix} = \frac{1}{E}\begin{bmatrix}1+Q(2\sigma_x-\sigma_\theta)^2 & -\upsilon+Q(2\sigma_x-\sigma_\theta)(2\sigma_\theta-\sigma_x)\\ -\upsilon+Q(2\sigma_x-\sigma_\theta)(2\sigma_\theta-\sigma_x) & 1+Q(2\sigma_\theta-\sigma_x)^2\end{bmatrix}\begin{Bmatrix}\dot\sigma_x\\ \dot\sigma_\theta\end{Bmatrix}, \tag{7}$$

where

$$Q = \begin{cases} 0, & \sigma_e \le \sigma_{e\max},\\ \dfrac{1}{4\sigma_e^2}\left(\dfrac{E}{E_t}-1\right), & \sigma_e > \sigma_{e\max}, \end{cases} \tag{8}$$

where $\dot{()}$ denotes an increment in (), σ_e is the equivalent stress, and $E_t = E_t(\sigma_e)$ is the tangent modulus of material. They are given as follows:

$$\sigma_e^2 = \frac{3}{2}S_{ij}S_{ij}, \tag{9}$$

$$\frac{1}{E_t} = \frac{1}{E}\left[1+\frac{3}{7}n\left(\frac{\sigma_e}{\sigma_y}\right)^{n-1}\right], \tag{10}$$

where

$$S_{ij} = \sigma_{ij} - \frac{1}{3}\sigma_{kk}\delta_{ij}, \tag{11}$$

where S_{ij} is the deviatoric stress tensor, σ_{ij} is the stress tensor, σ_{kk} is the first invariant of stress tensor, and δ_{ij} is the Kronecker Delta function.

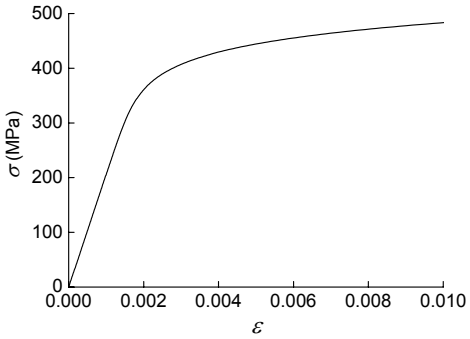

Fig. 2 Stress-strain curve for the Ramberg-Osgood model
σ_y=400 MPa, E=206 GPa, n=10.7

2.3 Principle of virtual work

According to the principle of virtual work, the equation below must be satisfied when the tube is in an equilibrium state:

$$2R\int_0^\pi\int_{-t/2}^{t/2}(\hat\sigma_x\delta\dot\varepsilon_x + \hat\sigma_\theta\delta\dot\varepsilon_\theta)\mathrm{d}\theta\mathrm{d}z = \delta\dot W, \tag{12}$$

where $(\hat{\bullet}) \equiv (\bullet + \dot{\bullet})$, and $\delta\dot{W}$ is the virtual work of the external loads, which can be given by

$$\delta\dot{W} = \hat{P}\delta\dot{V} + \hat{T}\delta\dot{\varepsilon}_x^0, \tag{13}$$

where $\delta\dot{V}$ is the change of volume per unit length of the tube considered. In expanded form, Eq. (12) becomes:

$$\begin{aligned} &2R\int_0^{\pi}\int_{-t/2}^{t/2}(\hat{\sigma}_x\delta\dot{\varepsilon}_x + \hat{\sigma}_\theta\delta\dot{\varepsilon}_\theta)\mathrm{d}\theta\mathrm{d}z \\ &= \hat{P}R\int_0^{2\pi}[\delta\dot{w} + (2\hat{w}\delta\dot{w} + 2\hat{v}\delta\dot{v} + \hat{w}\delta\dot{v}' \\ &\quad + \hat{v}'\delta\dot{w} - \hat{v}\delta\dot{w}' - \hat{w}'\delta\dot{v})/(2R)]\mathrm{d}\theta + \hat{T}\delta\dot{\varepsilon}_x^0. \end{aligned} \tag{14}$$

It is assumed that the deformations of the pipe cross-section, i.e., the in-plane displacements w and v, are symmetric about the axis θ=0, and they are the functions of θ. Therefore, w and v can be approximated by the following series expansions (Gellin, 1980):

$$w \cong R\sum_{n=0}^{N} a_n \cos(n\theta), \quad v \cong R\sum_{n=2}^{N} b_n \sin(n\theta). \tag{15}$$

Substituting Eq. (15) into Eq. (14), a series of $2N$+1 nonlinear algebraic equations in term of $\{\dot{a}_0, \dot{a}_1, \cdots, \dot{a}_N, \dot{b}_2, \dot{b}_3 \cdots \dot{b}_N, \dot{\varepsilon}_x^0\}$ may be obtained.

2.4 Solution method

The resultant $2N$+1 nonlinear algebraic equations are solved iteratively in the present solution. Some parameters should be prescribed in advance, namely geometric dimensions, material parameters, and load sizes. The number of Gaussian integral points, for the half cross-section of the tube, along the circumferential direction and through the thickness is k and l, respectively (Fig. 3).

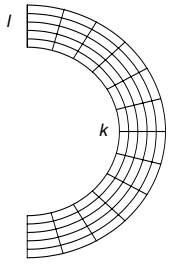

Fig. 3 Distribution of Gaussian integral points

The main steps of solution procedure for combined loading case are shown in Fig. 4. The tube can be loaded by axial tension T, curvature κ as well as external pressure P. The loading process is controlled by prescribing the increments of three loading parameters $\{\Delta T, \Delta P, \Delta\kappa\}$. When P is specified to zero, the case would be that of combined bending and tension. If the prescribed P and T both equal zero, it would reduce to the pure bending case.

The converged solution of the previous step is regarded as the initial estimate of nodal displacements for the next step. Subsequently, the strain increment can be obtained through the increments of nodal displacements and curvature, and then the stress increment can be achieved. Note that this procedure also involves nested iteration of the constitutive relationship. After obtaining the stress components of each integral point, the problem can be solved using the Newton-Raphson method. Strains, stresses as well as displacements corresponding to every integral point are updated when the converged solution is achieved.

After each converged solution, the moment can be obtained:

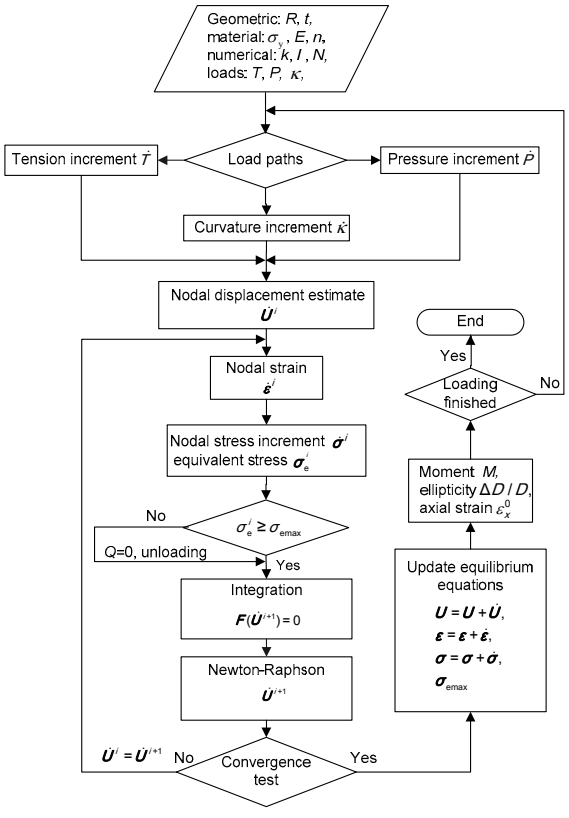

Fig. 4 Flow chart of numerical solution procedure

$$M = 2R\int_0^{\pi}\int_{-t/2}^{t/2}\sigma_x\varsigma\,\mathrm{d}\theta\mathrm{d}z. \tag{16}$$

It is found that the solution can meet the precision requirements when N equals 4 to 6. In the case of pure bending, k=12 and l=5 is sufficient. While for the combined case, the mesh should be finer, therefore, k=12 and l=7 is found to be adequate.

3 Numerical simulations

A finite element model is developed within the framework of the software ABAQUS to simulate the buckling behavior of pipes under simultaneous tension, bending, and external pressure. 3D, eight-node incompatible solid element, C3D8I, is chosen to model the pipe. Since this type of element is enhanced by incompatible modes to bending behavior, it is best suited for the present problem (Simo and Armero, 1992; Hibbitt *et al*., 2006). The J_2 flow theory of plasticity with isotropic hardening proposed by Corona *et al*. (2006) is adopted to describe the plastic behavior of material, and the Ramberg-Osgood constitutive model is used by multi-linear approximations of the stress-strain curve shown in Fig. 2.

The symmetry of the loads and deformations reduces the problem to a quarter of a pipe. As a result, symmetrical boundary conditions are applied at the mid-span (X=0) and Z=0 planes (Fig. 5). Besides, additional spring constraints along vertical direction (Y) are applied at the mid-span plane. This kind of elastic constraints is desirable for this problem since it can avoid the stress concentration phenomenon which is inevitable if rigid constraints are applied.

*KINEMATIC COUPLING relationship is imposed between the nodes on the right end of the tube and a reference point (the central node or the bottom one are both suitable). The right end plane is constrained to remain plane in the loading process, and at the same time the cross-section should be free to deform. The curvature is applied by prescribing the angle of rotation at the reference point, φ. Likewise, uniform tension is applied to the model through this reference point, and hydrostatic pressure is implemented on the external surface of the pipe. Thus, the average curvature of the section can be given by

$$\kappa = \varphi / L. \tag{17}$$

To facilitate the development of buckling deformation, the length of the pipe, L=3D is considered to be suitable. The pipe model is meshed into 6 parts through the thickness, 100 parts around the half circumference and 100 parts along the length, which is found to be adequate. Fig. 5 illustrates a typical finite element mesh used in the analyses. Furthermore, the Nlgeom option is selected for the nonlinear calculation, and the Riks algorithm (arch length method) is adopted here.

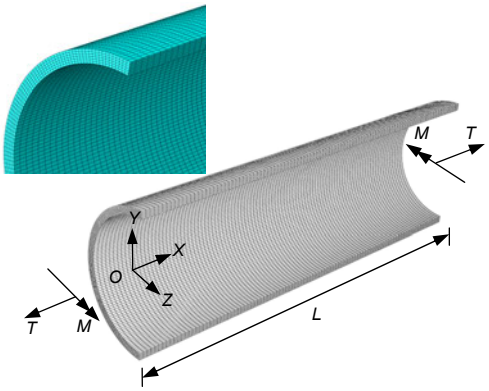

Fig. 5 Finite element mesh and loadings

4 Results and discussion

4.1 Illustrative example using theoretical formulations

The maximum curvature in the sag-bend region often occurs close to the seabed where the maximum water depth is reached. Considering that the curvature and hydrostatic pressure exerted on the pipes increases with the depth of the water, while axial tension is nearly maintained constant, the case of T→Radial(κ, P) loading path is examined.

The pipe is first tensioned incrementally to a chosen value T=1000 kN, and then curvature and external pressure are increased proportionately until the values of κ=0.15 and P=10 MPa are reached. The main features of the pipe response subjected to the combined loads are illustrated in Fig. 6 for a pipe with its diameter D=254 mm (10 inch) and D/t=20. The predicted ellipticity-water depth, ellipticity-curvature, axial strain-curvature, and moment-curvature curves

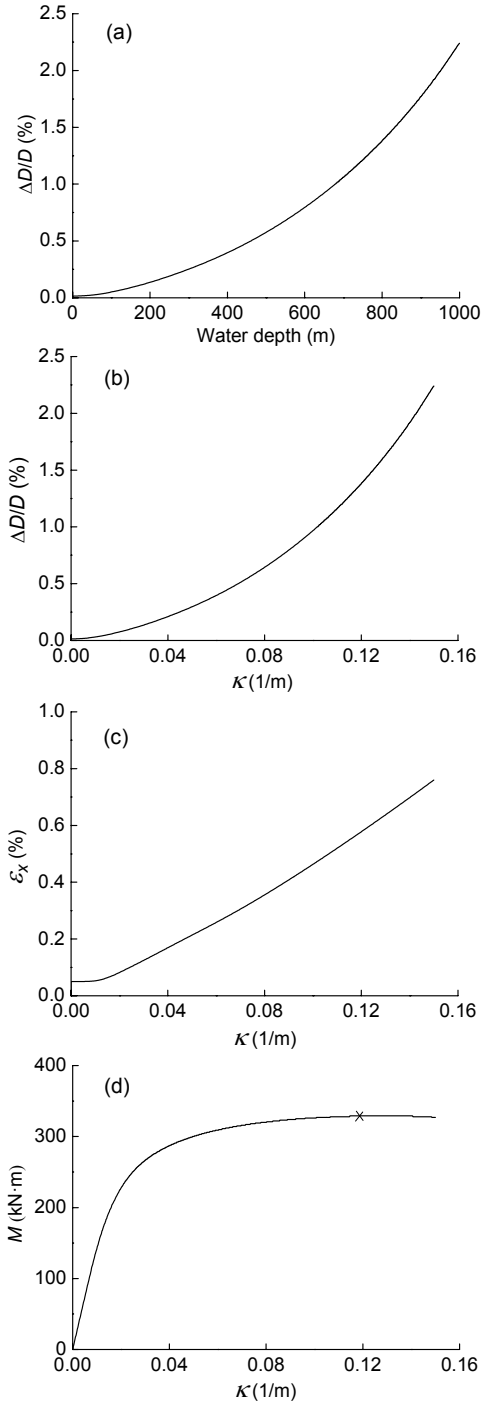

Fig. 6 Predicted responses for T→Radial(κ, P) loading path. σ_y=400 MPa, D/t=20, n=10.7
(a) Ellipticity-water depth; (b) Ellipticity-curvature; (c) Axial strain-curvature; (d) Moment-curvature

are shown in this figure. The increase of ellipticity is approximately proportional to the curvature and water depth at the beginning. However, the nonlinearity becomes more and more notable as the loads augment. As to the axial strain of the pipe, it nearly experiences a linear growth with curvature. In addition, it can be seen from moment-curvature response that there exhibits a limit moment before collapse. Once attaining the limit moment, localized deformation would quickly develop in a region of about 5 to 6 times of the tube diameters, which can be taken as the critical state of buckling.

4.2 Comparisons of finite element analysis results with theoretical solutions

Numerical simulations and theoretical calculations are carried out respectively for the scenario of Radial(T, P, κ) loading path. In other words, three loading parameters {ΔT, ΔP, $\Delta\kappa$} are simultaneously applied to the model. The analyses are performed for the pipe model based on the parameters of D=254 mm, D/t=20, n=10.7, σ_y=400 MPa, T=600 kN, P=35 MPa and κ=0.013. The sequences of deformed configuration and stress distribution during the loading process are depicted in Fig. 7.

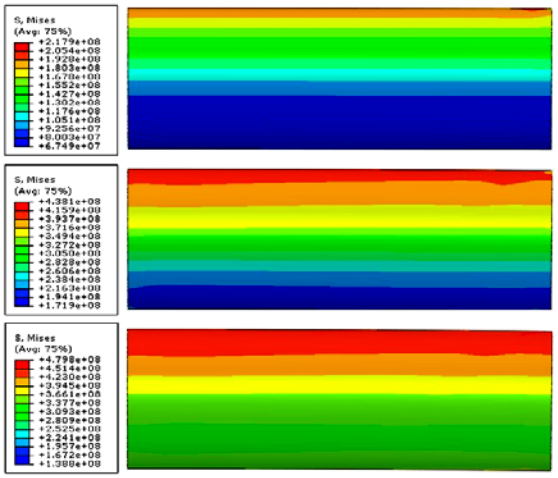

Fig. 7 Deformed configuration and stress distribution during loading process

The comparison of responses calculated by the two methods is shown in Fig. 8. The predicted ellipticity of two models is quite close in the elastic range. However, the increase of theoretical result slightly lags behind that of finite element simulation at high values of loadings.

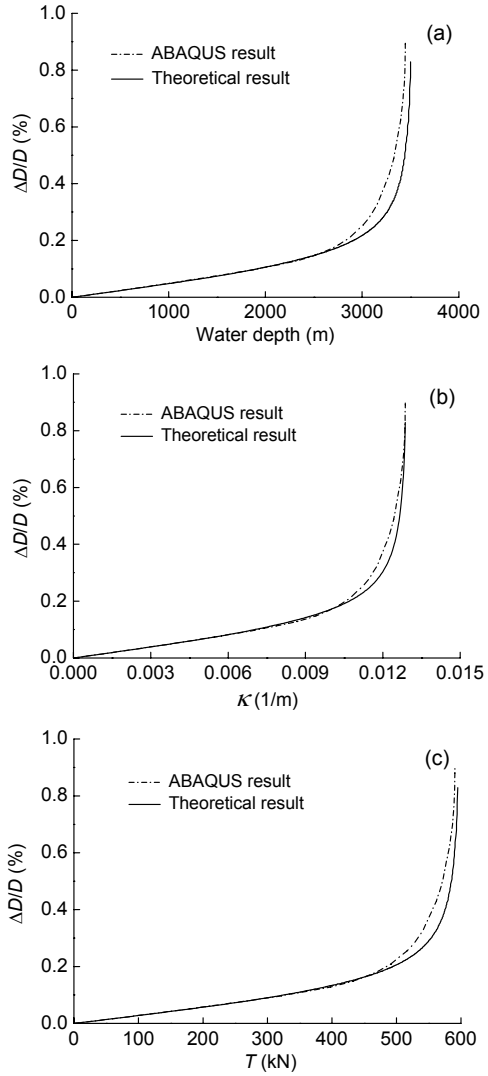

Fig. 8 Comparisons of finite element analysis results with theoretical solutions

(a) Ellipticity-water depth; (b) Ellipticity-curvature; (c) Ellipticity-tension

The main reason for the difference is that ABAQUS uses a finite deformation J_2 flow theory of plasticity whereas the theoretical formulation in Eqs. (7)−(11) is small deformation. In addition, the theoretical model simplifies this 3D problem to a 2D one, which only takes into account the stresses along the axial and circumferential directions. The disregard of the secondary radial stress and shear stress will not generate much error in the elastic range. However, with the increase of stress in the radial direction, the discrepancies become more and more notable. Moreover, due to the disregard of radial stress and shear stress, the equivalent stress will be smaller compared with the practical situation, hence, later occurrence of plastic plateau. Likewise, the growth of ellipticity is somewhat delayed. The suitability of the theoretical method used in predicting the buckling response of deepwater pipes has been validated herein.

4.3 Parametric study

The theoretical model is adopted to examine the effects of several important factors including tension T, strain-hardening parameter n, yield stress σ_y as well as diameter-to-thickness ratio D/t. $T\rightarrow$Radial(κ, P) is the loading path considered in the present section. Besides, some discussions and comparisons are made concerning the design of pipes in engineering practice.

The buckling of tube is related to several factors, such as the diameter D, wall-thickness t, material properties, initial ellipticity $\Delta D/D$, and load history. In addition, residual stress induced in the manufacturing process as well as yield anisotropy play an important role in the occurrence of tube buckling. For offshore applications, a D/t value ranging from 10 to 70 is recommended. While for deepwater application, a D/t value ranging from 10 to 35 is more suitable. In addition, the yield strength of steel for typical offshore pipelines is commonly between 276 and 448 MPa. Besides, the tubes, with initial ellipticity exceeding 0.5%, should be avoided in the deepwater applications (Ju and Kyriakides, 1991).

Figs. 9 and 10 show that axial tension has a significant effect on bending moment carrying capacity of a pipe. The tension is prescribed to 500, 1000 and 1500 kN respectively, and the ratio of $(P/P_0):(\kappa/\kappa_0)$ ranges from 5:1, 1:1, 1:3 to 1:8, respectively denoted as Radial 1–Radial 4, which consists of 12 different load combinations. The result indicates that the presence of tension impairs bending moment carrying capacity greatly. With the increase of tension applied, the limit moment M_c drops. Furthermore, it can also be observed that the increase of external pressure will cause the value of limit moment to decrease. Additionally, as can be seen in Fig. 10, the predicted critical pressure P_c and critical curvature κ_c become smaller when the value of tension increases. It is important to note that the results are normalized to dimensionless factors by the following variables:

$$M_0=\sigma_0 D_0^2 t,\ \ P_0=2\,\sigma_0 t/D_0,\ \ \kappa_0=t/D_0^2, \quad (18)$$

where mean diameter D_0=D−t, and σ_0 is API yield stress (API, 2004), i.e., the stress at a strain of 0.005.

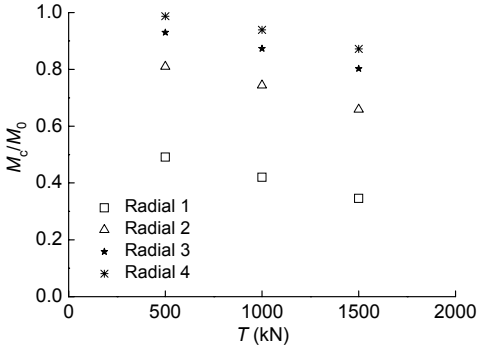

Fig. 9 Limit moment versus applied tension

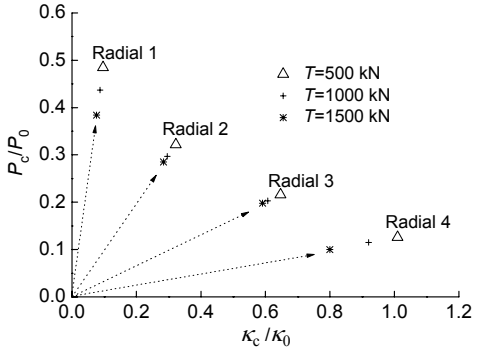

Fig. 10 Effects of tension on critical pressure and curvature

Fig. 11 shows how the critical pressure and critical curvature vary with the material yield stress σ_y with other parameters kept constant. Clearly, the tubes with larger yield stress possess higher critical pressure and curvature. In addition, it is also worth noting that at higher curvatures the effect of yield stress is less pronounced compared with the cases of lower curvatures.

Larger strain-hardening parameter n means larger strain-hardening effect. Fig. 12 presents the variation of critical pressure and critical curvature with the strain-hardening parameter n. It can be observed that tubes with larger n can sustain larger critical pressure and curvature, i.e., higher load-carrying capacity.

The effect of diameter-to-thickness ratio D/t on the critical pressure and curvature is examined in Fig. 13. Three D/t values 15, 20 and 25 are adopted, while keeping other parameters constant. Just as expected, the limit values corresponding to lower D/t tubes are higher than those of larger D/t ones. In addition, note that the degree of its influence varies with different combinations of loads applied.

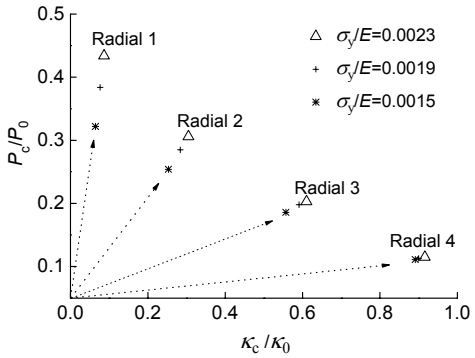

Fig. 11 Effects of yield stress on critical pressure and curvature

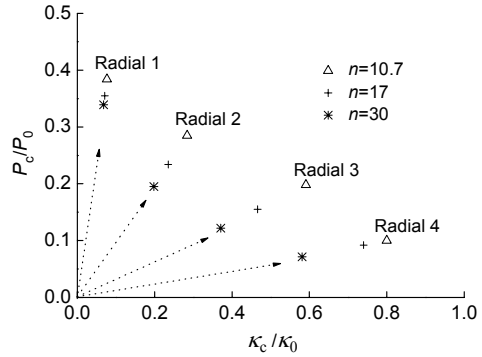

Fig. 12 Effects of strain-hardening parameter on critical pressure and curvature

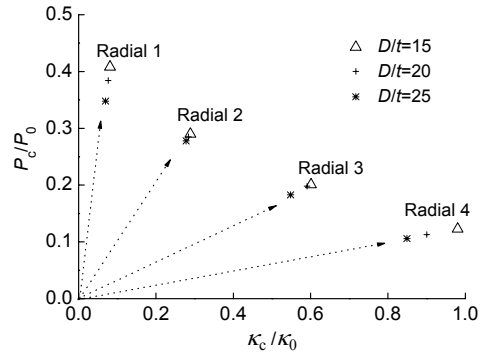

Fig. 13 Effects of D/t on critical pressure and curvature

5 Conclusions

The buckling behavior of the pipes under T→Radial(κ, P) load path is presented in the fact that this load path could approximate the loading history experienced by the pipeline in the sagbend region for deepwater pipe-laying operation. Comparisons between the results of theoretical analysis and those of numerical simulations demonstrate that the theoretical formulation can accurately predict the buckling behavior of deepwater pipes under simultaneous tension, bending, and external pressure.

A series of parametric study on the buckling response of deepwater pipes subjected to T→Radial (κ, P) load path is conducted adopting the theoretical formulation developed. The following conclusions can be drawn.

1. The load-carrying capacity of the tube is significantly affected by the tension applied. With the increase of tension, the limit moment obviously drops, and the predicted critical pressure and curvature would become smaller. In the case of equal proportional loading between external pressure and curvature, the effect of tension on load-carrying capacity of the tube is less conspicuous compared with other loading ratio.

2. The buckling behavior and load-carrying capacity of pipes is quite sensitive to material properties. Larger yield stress σ_y and strain-hardening parameter n always lead to higher limit pressure and curvature, i.e., stronger resistance to pipe buckling. The critical pressure of the pipe is more susceptible to yield stress rather than strain-hardening parameter, whereas the critical curvature is just the contrary. Therefore, the high strength steel is preferred to improve the resistance to external pressure for deepwater pipes in the practical engineering.

3. Diameter-to-thickness ratio D/t plays a very important role in buckling response of pipes. In general, pipes with lower D/t values possess stronger capability to resist the buckling deformation. But, the degree of its influence varies with different combination of loads applied.

In summary, it can be concluded that the theoretical formulation and solution method described in this context could provide a reasonably-accurate estimate of the buckling and collapse of deepwater pipes. In addition, it should be mentioned that experiments under simultaneous tension, bending, and external pressure should be carried out, and thus, the effectiveness of this theoretical method can be carefully examined.

References

Al-Sharif, A.M., Preston, R., 1996. Simulation of Thick-Walled Submarine Pipeline Collapse under Bending and Hydrostatic Pressure. Proceedings of Offshore Technology Conferences, Houston, Texas, USA, OTC8212, p.589-598.

API (American Petroleum Insitute), 2004. API Specifications 5L: Specifications for Line Pipe (43rd Ed.). API Publishing Services, Washington DC, USA.

Bai, Y., Igland, R.T., Moan, T., 1997. Tube collapse under combined external pressure, tension and bending. *Marine Structures*, **10**(5):389-410. [doi:10.1016/S0951-8339(97)00003-8]

Corona, E., Kyriakides, S., 1988. On the collapse of inelastic tubes under combined bending and pressure. *International Journal of Solids and Structures*, **24**(5):505-535. [doi:10.1016/0020-7683(88)90005-4]

Corona, E., Lee, L.H., Kyriakides, S., 2006. Yield anisotropy effects on buckling of circular tubes under bending. *International Journal of Solids and Structures*, **43**(22-23):7099-7118. [doi:10.1016/j.ijsolstr.2006.03.005]

Dyau, J.Y., Kyriakides, S., 1992. On the response of elastic-plastic tubes under combined bending and tension. *Journal of Offshore Mechanics and Arctic Engineering*, **114**(1):50-62. [doi:10.1115/1.2919952]

Gellin, S., 1980. Plastic buckling of long cylindrical shells under pure bending. *International Journal of Solids and Structures*, **16**(5):397-407. [doi:10.1016/0020-7683(80)90038-4]

Hibbitt, H.D., Karlsson, B.I., Sorensen, P., 2006. ABAQUS Theory Manual, Version 6.3. Pawtucket, Rhode Island, USA.

Ju, G.T., Kyriakides, S., 1991. Bifurcation buckling versus limit load instabilities of elastic-plastic tubes under bending and external pressure. *Journal of Offshore Mechanics and Arctic Engineering*, **113**(1):43-52. [doi:10.1115/1.2919895]

Kashani, M., Young, R., 2005. Installation load consideration in ultra-deepwater pipeline sizing. *ASCE Journal of Transportation Engineering*, **131**(8):632-639. [doi:10.1061/(ASCE)0733-947X(2005)131:8(632)]

Kyriakides, S., Shaw, P.K., 1982. Response and stability of elastoplastic circular pipes under combined bending and external pressure. *International Journal of Solids and Structures*, **18**(11):957-973. [doi:10.1016/0020-7683(82)90086-5]

Kyriakides, S., Corona, E., 2007. Mechanics of Offshore Pipelines, Volume 1: Buckling and Collapse. Elsevier Science, Oxford, UK and Burlington, Massachusetts.

Li, Z.G., Wang, C., He, N., Zhao, D.Y., 2008. An overview of deepwater pipeline laying technology. *China Ocean Engineering*, **22**(3):521-532.

Simo, J.C., Armero, F., 1992. Geometrically non-linear enhanced strain mixed methods and the method of incompatible modes. *International Journal for Numerical Methods in Engineering*, **33**(7):1413-1449. [doi:10.1002/nme.1620330705]

Yuan, L., Gong, S.F., Jin, W.L., Li, Z.G., Zhao, D.Y., 2009. Analysis on buckling performance of submarine pipelines during deepwater pipe-laying operation. *China Ocean Engineering*, **23**(2):303-316.